Energy Preservation of High-Order Mimetic Differences for Systems of Conservation Laws

Miguel A. Dumett, Johnny Corbino, and Jose E. Castillo

December 27, 2023

Publication Number: CSRCR2023-11

Computational Science & Engineering Faculty and Students Research Articles

Database Powered by the Computational Science Research Center Computing Group & Visualization Lab

COMPUTATIONAL SCIENCE & ENGINEERING

SAN DIEGO STATE UNIVERSITY

Computational Science Research Center
College of Sciences
5500 Campanile Drive
San Diego, CA 92182-1245
(619) 594-3430

Energy Preservation of High-Order Mimetic Differences for Systems of Conservation Laws *

Miguel A. Dumett † Johnny Corbino ‡ Jose E. Castillo §

December 27, 2023

Abstract

In this paper, we prove energy conservation of high-order mimetic difference schemes for linear and nonlinear systems of conservation laws. We aim to conservation laws were the flux is given by the gradient of some potential field. Furthermore, we numerically validate the theoretical foundation of our approach by showing that high-order mimetic schemes converge to the exact solution of general nonlinear systems of conservation laws preserving all quantities of interest.

1 Introduction

Roughly, a partial differential equation (PDE) is an equation that involves an unknown function of two or more variables and some of their partial derivatives. The goal of PDE theory is, ideally, to solve for the unknown function and/or to determine some properties of such a solution. The variety of application areas where PDE equations are used to model phenomena, glimpses that a general theory might not exist and naturally guides PDE researchers to focus on particular PDEs. Theoretical approaches for solving classes of PDEs attempt to find solutions that are unique and that change smoothly if the conditions specified in the PDE change a little. When this is possible a PDE is called well-posed. When the solution of a PDE does have a solution that is differentiable with continuity at least up to the highest partial derivative degree present in the PDE, the solution is called classic. However, in general, such a PDE solution does not exist. Still, one might be able to introduce the notion of generalized or weak solutions and prove that the PDE is well-posed when one targets these non-classical solutions.

*This work was partially supported by SDSU.

†Computational Science Research Center at the San Diego State University (mdumett@sdsu.edu).

‡Lawrence Berkeley National Laboratory (jcorbino@lbl.gov).

§Computational Science Research Center at the San Diego State University (jcastillo@sdsu.edu).

One example of a PDE that illustrates the need to introduce generalized solutions and that is utilized to model phenomena in fluid mechanics is a scalar conservation law. This PDE model often shows the formation and propagation of a discontinuous solution (called a shock wave). Conservation laws are an example of first-order PDEs. First-order PDEs can be transformed, at least locally, by the method of characteristics, into a system of ordinary differential equations (ODEs), and sometimes explicitly solved locally. In the case of PDE scalar conservation laws, it can be shown that the projected characteristics are propagation lines, whose slopes are given by the derivative of the flux term of the PDE, where the solution is constant. The presence of initial conditions where two points have different derivatives may imply that the projected characteristic could cross, generating shock waves at a certain future time. Before that time, energy conservation of the initial condition holds.

Researchers in different application areas have recognized, that numerical methods for PDEs that preserve crucial properties of them, namely, symmetries, conserved quantities, etc., are usually more precise than those that do not [25, 27]. For example, it is clear that some properties of the numerical flux are key to ensuring the recovery of the entropy solution. In particular, numerical schemes should mimic the properties of the continuum problem to ensure that the computed solution converges to a weak entropy solution to the system of conservation laws.

Mimetic methods aim to preserve these features. This collection of techniques can be divided into two groups. The most traditional mimetic approach attempts to enforce some vector calculus integral identities and from them derive some consequences that will characterize the discrete analogs of the divergence, gradient, curl and Laplacian differential operators [25, 3, 5, 27]. The second one, the most recent development, is composed of those called fully mimetic, which target to reproduce vector [24], tensor [27, 18], and/or exterior [1, 15, 18, 17] calculi identities, as well as algebraic topology exact sequences [12, 13].

Nevertheless, trying to replicate characteristics of the solution is not exclusive of mimetic methods. Among the non-mimetic methods which display some level of mimicking these properties, one finds the cell method in electromagnetism [20], the covolume method for the Navier-Stokes and Maxwell's equations [21], the summation by parts methods in mixed hyperbolic-parabolic problems [22, 23], the finite volume method for the heat equation [10, 11], the mixed finite element method [2], as well others, among which one finds monotone schemes (finite-differences, finite volume, etc.), and higher-order accurate techniques, such as essentially non-oscillatory (ENO) schemes, and weighted essentially non-oscillatory (WENO) methods, discontinuous Galerkin, finite elements, spectral methods, as well as others [16].

This paper is about high-order mimetic differences (MD), one of the traditional mimetic methods. MD was the first mimetic method to achieve high-order operators. Moreover, the order of accuracy is uniform over the whole domain, including the boundary, a feature that

no other mimetic techniques shares. Distinguishing it from other traditional mimetic methods demands giving more background for this class of methods as a group and providing more detail about the differences amid distinctive traditional mimetic approaches.

For, these techniques construct discrete analogs of the spatial first-order differential divergence, gradient, and curl operators, that mimic vector and tensor calculus integral identities (the Gauss divergence or the Green's or Stokes' theorems or their generalizations via Green's identities), by utilizing convenient weighted inner products.

The first ideas of mimetic methods were developed by A.A. Samarskii and his group in the Soviet Union during the fifties and sixties of the twentieth century, and their arrival to the West during the seventies and eighties. Currently, three different collections of mimetic methods have been developed. In historical precedence,

1. the support-operator methods [25]: originally developed by the T-7 group in Los Alamos National Laboratory (LANL), it uses some vector/tensor calculus integral identities to define the primal operator according to the PDE (one among the divergence, gradient, and curl operators), and the others (as dual operators) via duality relationships from Green's identities, on staggered grids. These techniques construct operators are of low-order accuracy.

2. the high-order mimetic differences [3, 5]: originally developed at San Diego State University, by J.E. Castillo group at the Computational Science Research Center, Castillo-Grone (2003), and Corbino-Castillo (2020), focuses on high-order accuracy representations of the divergence, gradient, and curl operators, as well as weighted inner products and interpolation operators, that are fixed obtained from an extension of the Gauss' divergence theorem, independently of the PDE, and whose accuracy is uniform over the whole staggered grid, and,

3. the mimetic finite differences (MFD) [27]: a collaboration between LANL and a research group in Milano-Pavia, Italy. Primal and dual versions for all (divergence, gradient, and curl) operators that satisfy all integral theorems of vector calculus, are constructed for general polyhedral and polygonal elements in a finite element style, where high-order accuracy is achieved by adding nodes in each element.

As principal differences, one can find that high-order mimetic differences define all mimetic operators on cell centers and/or faces but not on nodes, while support-operator and MFD work on nodes, edges, faces and centers. In addition, support-operator and high-order mimetic differences define the operators across several cells while MFD does it in an element-wise fashion.

This work focuses on demonstrating energy conservation of Corbino-Castillo [5] high-order mimetic differences (even though a similar proof can be elaborated for the Castillo-Grone [3] approach) when applied to conservation laws where solutions are understood in the

classical sense. In addition, a mimetic scheme is proposed for numerically solving some conservation laws, and proof of the convergence of this mimetic scheme is shown.

High-order mimetic differences are numerical schemes that construct partial differential equation (PDE) discrete analogs based on matrix representation of spatial differential operators, like the divergence, gradient, and Laplacian. These mimetic methods differ from the ones that originally appeared [25] in their high-order of accuracy, which is achieved by the introduction of divergence and gradient weight matrices P and Q and the mimetic operators are constructed independently of each other.

Mimetic difference discrete analogs keep uniform accuracy order over the whole discrete domain, usually a staggered grid where discrete scalar and vector fields are defined on different points [3, 4, 5]. Information from the discrete scalar and vector fields is passed from/to different points by utilizing high-order mimetic interpolation operators [7, 8].

Mimetic differences operators mimic properties of the continuum problem and their discrete analogs satisfy discrete integral versions of the vector calculus identities. This is a consequence of satisfying a discrete analog of the one-dimensional (1D) integration by parts formula and its extension to 3D named extended Gauss divergence theorem [8].

It has been shown that mimetic schemes for the three-dimensional (3D) advection equation can preserve energy and when combined with an energy-preserving time integration scheme, the mimetic scheme converges [9].

Mimetic difference schemes based on the Castillo-Grone operators and the Corbino-Castillo operators have been used effectively to solve a variety of problems over the years. Some of them that cover a wide range of problems can be found in [28, 29, 33, 30, 31, 32, 34].

In this work, conservation laws are understood as systems of linear/nonlinear first-order hyperbolic PDEs in several variables (d dimensions), written in divergence or non-divergence form. These models are written in terms of, for example, c conserved quantities u in some physical region $U \subset \mathbb{R}^d$ under investigation. The conservation properties typically assert that the rate of change of the quantities of interest is governed by a flux function, that controls the loss or gain rate of u through the boundary of U.

The choice of the conservation laws that are targeted for demonstrating the energy conservation of the mimetic discrete analogs in this paper, obeys both,

1. the possibility of applying the extended divergence Gauss theorem by mimetic difference property, and

2. the fact that a mathematical understanding of a general system of conservation laws is not available for $c \geq 1$, and $d \geq 1$.

Moreover, for the following cases of conservation laws, the previous conditions hold:

1. Symmetric hyperbolic systems of first-order PDEs (with constant coefficients). This is an example of one ($c = 1$) linear conservation law in $d \geq 1$ dimensions. The system can be solved utilizing the Fourier transform. When the coefficients are non-constant energy methods and the vanishing viscosity technique guarantees the existence a uniqueness of a weak solution ([14] pp 402-412).

2. Scalar conservation law in one space dimension with potential flux. Even though it is known that in general the method of characteristics demonstrates that it is not possible to find a smooth solution that exists for all positive times ([14] pp. 97-136), for an "exact" flux it can be shown that it is true. Nevertheless, for a convex, smooth flux that satisfies entropy conditions, and bounded initial conditions, the Lax-Oleinik formula is a weak solution of the conservation law, which is unique if it is an entropy solution. This is an example of one ($c = 1$) nonlinear scalar ($d = 1$) conservation law.

3. Finally, leveraging from the two previous cases, it is considered the case of a system of nonlinear PDEs, for a potential flux. Even though it is known that in general the Darboux method, for local existence and uniqueness of solutions of first-order PDE systems, does not guarantee the existence and uniqueness of a weak solution for any positive time, this is true for "exact" fluxes. This is an example of several nonlinear conservation laws ($c \geq 1$) in $d \geq 1$ dimensions.

In Section 2, the system of c conservation laws in $\mathbb{R}^d$ is introduced, and using Corbino-Castillo operators, it is demonstrated that mimetic difference discrete analog schemes conserve energy.

Mimetic differences discrete analogs are first obtained for one linear conservation system in $d \geq 1$ dimensions, since for some symmetric positive-definite matrices, the exact solution is known.

Before starting the proof for this system of conservation laws, some preliminaries that will be utilized in all discrete analog energy conservation proofs, are presented. Then, the energy-preserving proof is exhibited.

In particular, the focus is on explicitly displaying the matrix representation of the multi-dimensional versions of the mimetic operators (divergence, divergence quadrature weight, and divergence interpolation). Similar expressions, for the multi-dimensional versions of the gradient, gradient quadrature weight, and gradient interpolation, even though not shown, are also available. The 3D versions of all the mimetic operators mentioned can be found in [8].

After that, mimetic discrete analogs are constructed for some nonlinear scalar flux ($c = 1, d = 1$), and their energy-preserving property is demonstrated.

Finally, leveraging from the two previous cases, a mimetic discrete analog is proposed for some system of conservation laws ($c \geq 1$) in $d \geq 1$ dimensions [14], and its energy

conservation property is shown.

In Section 3, we numerically integrate a system of conservation laws and discuss our results. These two properties are utilized to show the numerical convergence of the spatial differential mimetic operator analogs when combined with a time integration scheme for conservation laws.

Lastly, we present our conclusions in Section 4.

2 Energy conservation of mimetic analogs of some systems of conservation laws

In this section, it is shown that mimetic analogs of some systems of conservation laws conserve energy.

2.1 The system of conservation laws

Consider the following initial-value problem for a general system of conservation laws:

$$\begin{aligned} u_t + \nabla \cdot F(u) &= 0, \quad (x,t) \in U \times (0,\infty), && (1) \\ u &= u_0, \quad (x,t) \in U \times \{0\}, && (2) \end{aligned}$$

where $U \subset \mathbb{R}^d$ is a smooth and bounded region, $u = u(x,t) = (u^1(x,t), \cdots, u^c(x,t))$, for $x \in U$, $t \geq 0$, and F the flux function is such $F : \mathbb{R}^c \mapsto \mathbb{M}^{c \times d}$ (the latter the set of matrices of order $c \times d$), and $u_0 = (u_0^1, \cdots, u_0^c)$ is the initial condition of $u = (u^1, \cdots, u^c)$.

2.2 Case I: Symmetric hyperbolic systems of first-order PDEs with constant coefficients

Mathematical understanding of problem (1)-(2) is not available [14, p. 568]. Instead, consider the initial-boundary value problem for the system of $c = 3$ conservation laws in two dimensions ($d = 2$), the shallow water equations linearized around a constant velocity field (a, b) [26, p. 217]:

$$\begin{aligned} u_t + a u_x + b u_y + h_x &= 0, \\ v_t + a v_x + b v_y + h_y &= 0, \\ h_t + a h_x + b h_y + u_x + v_y &= 0. \end{aligned} \qquad (3)$$

It can be shown that the eigenvalues of this system are purely imaginary and so, the system is hyperbolic and well-posed [26, p. 218].

In (3),

$$F\begin{pmatrix} u \\ v \\ h \end{pmatrix} = \begin{bmatrix} au+h & bu \\ av & bv+h \\ ah+u & bh+v \end{bmatrix} = \begin{bmatrix} F_1\begin{pmatrix} u \\ v \\ h \end{pmatrix} & F_2\begin{pmatrix} u \\ v \\ h \end{pmatrix} \end{bmatrix} = \begin{bmatrix} A_1\begin{pmatrix} u \\ v \\ h \end{pmatrix} & A_2\begin{pmatrix} u \\ v \\ h \end{pmatrix} \end{bmatrix},$$

with $F = [F_1, F_2], F_i : \mathbb{R}^c \mapsto \mathbb{R}, F_i(u, v, h)^T = A_i(u, v, h)^T$, $i = 1, 2$, and

$$A_1 = \begin{bmatrix} a & 0 & 1 \\ 0 & a & 0 \\ 1 & 0 & a \end{bmatrix}, \quad A_2 = \begin{bmatrix} b & 0 & 0 \\ 0 & b & 1 \\ 0 & 1 & b \end{bmatrix}.$$

If one defines $w = (u, v, h)^T$, then (3) can be written as

$$\begin{aligned} w_t + \nabla \cdot F(w) &= w_t + div\ (F_1(w), F_2(w)) \\ &= w_t + F_1(w)_x + F_2(w)_y \\ &= w_t + A_1 w_x + A_2 w_y = 0. \end{aligned}$$

Instead of the shallow water equations, consider a more general problem that has the same structure but with any symmetric (like in the previous example) constant matrices A_1, A_2 such (1) is a well-posed hyperbolic system. In other words, for general A_1, A_2, we assume a shallow water-like system whose matrix

$$R(z_1, z_2) = -i(A_1 z_1 + A_2 z_2),$$

with $z_1, z_2 \in \mathbb{R}^2$, has eigenvalues with non-negative real part [26, p. 200].

Furthermore, for $U = (-1, 1)^d$, this more general system can be extended to a system with c conservation laws in d dimensions (where A_i, $i = 1, \cdots, d$, are symmetric matrices),

$$w_t + A_1 w_{x_1} + \cdots + A_d w_{x_d} = 0, \qquad x \in (-1, 1)^d,\ t > 0, \tag{4}$$

$$w(x_1, \cdots, x_d, 0) = w_0(x_1, \cdots, x_d), \quad x \in (-1, 1)^d, \tag{5}$$

$$w(x_1, \cdots, x_{i-1}, -1, x_{i+1}, \cdots, x_d, t) = g_i(\hat{x}_i, t), \qquad \hat{x}_i \in [-1, 1]^{d-1}, \tag{6}$$

in which $w = (w_1, \cdots, w_c)$, $w_i = w_i(x_1, \cdots, x_d, t)$, $i = 1, \cdots, c$, and we assume that the boundary functions $g_i : \mathbb{R}^{d-1} \times (0, \infty) \mapsto \mathbb{R}^c$, $i = 1, \cdots, d$, have spatial coordinates defined on $\hat{x}_i = (x_1, \cdots, x_{i-1}, x_{i+1}, \cdots, x_d)$, and

$$F = [F_1, \cdots, F_d] = [A_1, \cdots, A_d], \quad A_i \in \mathbb{R}^{c \times c},\ i = 1, \cdots, d,$$

such, matrix

$$R(z_1, \cdots, z_d) = -\imath(A_1 w_1 + \cdots + A_d),$$

with $z_1, \cdots, z_d \in \mathbb{R}^d$, has eigenvalues with non-negative real part. A particular case, is when matrices A_i, $i = 1, \cdots, d$, are non-negative definite.

Notice that (4) is a conservation law not written in divergence form. It is well known that for $U = \mathbb{R}^n$, one can apply the Fourier transform to solve the constant coefficient initial value problem (1)-(2) and find that the exact solution is

$$w(x,t) = \frac{1}{(2\pi)^{n/2}} \int_{\mathbb{R}^n} e^{\imath\, x\cdot y}\, e^{-\imath t A(y)} \hat{w}_0(y)\, dy,$$

where $x = (x_1, \cdots, x_n)$ and $A(y) = \sum_{j=1}^{n} y_j A_j$ has for each $y = (y_1, \cdots, y_n) \in \mathbb{R}^n$, n real eigenvalues.

From now on, assume a well-posed system (4)-(6).

2.3 Preliminaries

Here, some common preliminaries to all mimetic scheme discrete analog energy-preserving proofs are introduced.

2.3.1 The d-dimensional continuous problem

By multiplying (4) by vector field w^T and integrating over U, one obtains

$$\int_U w^T w_t\, dX + \int_U \left(\sum_{i=1}^{d} w^T A_i w_{x_i} \right)\, dX = 0, \tag{7}$$

with dX the Cartesian volume element $dx_1 \cdots dx_d$.

The first and second terms in (7) verify

$$\begin{aligned}
\int_U w^T w_t\, dX &= \int_U \frac{1}{2}\, \frac{d(w^T w)}{dt}\, dX = \frac{1}{2}\, \frac{d}{dt} \left(\int_U w^T w\, dX \right), \\
\int_U \left(\sum_{i=1}^{d} w^T A_i w_{x_i} \right)\, dX &= \frac{1}{2} \int_U \left(\sum_{i=1}^{d} \frac{\partial}{\partial x_i} (w^T A_i w) \right)\, dX \\
&= \frac{1}{2} \int_U \nabla \cdot (w^T A_1 w, \cdots, w^T A_d w)\, dX.
\end{aligned}$$

After time integration from 0 to T, (7) becomes

$$\int_U [w^T(x,T) w(x,T) - w^T(x,0) w(x,0)]\, dX + \int_0^T \int_U \nabla \cdot (w^T A_1 w, \cdots, w^T A_d w)\, dX\, dt = 0, \tag{8}$$

where $x = (x_1, \cdots, x_d)$.

2.3.2 The d-dimensional staggered grid

Now, let us look at the discrete analog of (8) according to the Corbino-Castillo mimetic method [5].

Let m_i be the number of cells along the x_i axes, $i = 1, \cdots, d$. On the axes-uniform staggered grid $S = S_{m_1} \times \cdots \times S_{m_d}$, where

$$S_p = \{-1 = s_0, s_{\frac{1}{2}}, \cdots, s_{p-\frac{1}{2}}, s_{p+1} = 1\},$$

with $s_{j-\frac{1}{2}} = -1 + (j - \frac{1}{2})h_p$, $h_p = \frac{2}{p}$, $j = 1, \cdots, p$, define $U(s_{i_1}, \cdots, s_{i_d}, t)$, the Corbino-Castillo mimetic numerical approximation of $u(x_{i_1}, \cdots, x_{i_d}, t), s_{i_j} = x_{i_j}$, $j = 1, \cdots, d$, $i = 1, \cdots, m_i$.

In addition, define $W(t) = W(S_{m_1}, \cdots, S_{m_d}, t)$, the numerical approximation on grid S at time t, and the discrete element volume $h = h_{m_1} \cdots h_{m_d}$. Notice that $W(0) = w_0$.

For the approximation of a vector field, it is convenient to define the grid

$$N = \cup_{i=1}^{d}(N_{m_1} \times \cdots \times N_{m_{i-1}} \times S_{m_i} \times N_{m_{i+1}} \times \cdots \times N_{m_d}),$$

the middle edges of the voxels with centers at $S^0_{m_1} \times \cdots \times S^0_{m_n}$, where

$$N_q = \{r_1, \cdots, r_{q-1}\},$$

with $r_j = -1 + j\, h_q$, $h_q = \frac{2}{q}$, $j = 1, \cdots, q-1$, and $S^0_p = S_p \setminus \{s_0, s_{p+1}\}$.

In mimetic differences, approximations of scalar fields are defined on S, while approximations of vector fields are defined on N.

2.3.3 The discrete energy

Since there are no divergence or gradient operators in the volume integral $\int_U w^T \cdot w \, dX$ at time t, it is approximated by

$$h\,(\mathrm{vec}_L(W_1(t)), \cdots, \mathrm{vec}_L(W_c(t)))^T(\mathrm{vec}_L(W_1(t)), \cdots, \mathrm{vec}_L(W_c(t))),$$

with vec_L is the vectorization operator of the d-dimensional tensor $W_i(t)$, $i = 1, \cdots, c$, that maps $W_i(t)$ onto a vector of length $m = (m_1 + 2) \cdots (m_d + 2)$, following the lexicographic ordering.

Observe that for the scalar field, $\int_U w^T w(x_1, \cdots, x_d, t)\, dX$ is called the energy at time t, and one can define the discrete energy $\mathcal{E}$ of $W(t)$ at time t by

$$\mathcal{E}(t) = h\,(\mathrm{vec}_L(W_1(t)), \cdots, \mathrm{vec}_L(W_c(t)))^T(\mathrm{vec}_L(W_1(t)), \cdots, \mathrm{vec}_L(W_c(t))).$$

2.3.4 Some mimetic operators in d-dimensions

The d-dimensional order k, $k = 2, 4, 6, 8$, divergence interpolation operator that maps S onto N is

$$\mathcal{I}_D^k = \begin{bmatrix} \hat{I}_{m_d}^T \otimes \cdots \otimes \hat{I}_{m_2}^T \otimes I_{D_{x_1}}^k & & & \\ & \hat{I}_{m_d}^T \otimes \cdots \otimes \hat{I}_{m_3}^T \otimes I_{D_{x_2}}^k \otimes \hat{I}_{m_1}^T & & \\ & & \ddots & \\ & & & I_{D_{x_d}}^k \otimes \hat{I}_{m_{d-1}}^T \otimes \cdots \otimes \hat{I}_{m_1}^T \end{bmatrix},$$

with $I_{D_r}^k$, $r = x_1, \cdots, x_d$, the 1D interpolation operator on the r-axis [7], and

$$\hat{I}_p = \begin{bmatrix} 0 & \cdots & \\ 1 & & \\ & \ddots & \\ & & 1 \\ & \cdots & 0 \end{bmatrix},$$

the extension of the identity matrix by adding two extra rows of zeros (one at the top and one at the bottom). Notice that the $\mathcal{I}_D^k \in \mathbb{R}^{b \times m}$, where

$$b = (m_1 + 1)m_2 \cdots m_d + m_1(m_2 + 1)m_3 \cdots m_d + \cdots + m_1 \cdots m_{d-1}(m_d + 1),$$

is the cardinality of mimetic discrete vector fields in d dimensions, and $m = (m_1 + 2) \cdots (m_d + 2)$ is the cardinality of mimetic discrete scalar fields in d dimensions.

The weight matrix for the d-dimensional divergence operator is

$$\mathcal{Q}^k = \begin{bmatrix} I_{m_d+2} \otimes \cdots \otimes I_{m_2+2} \otimes Q_{m_1+2}^k & & \\ & \ddots & \\ & & Q_{m_d+2}^k \otimes I_{m_{d-1}+2} \otimes \cdots \otimes I_{m_1+2} \end{bmatrix},$$

where Q_p^k is the $p \times p$ weight matrix for the 1D divergence operator, and I_p the $p \times p$ identity matrix.

The d-dimensional divergence operator of order k is

$$D_{x_1 \cdots x_d}^k = \begin{bmatrix} \hat{I}_{m_d} \otimes \cdots \otimes \hat{I}_{m_2} \otimes D_{x_1}^k, & \hat{I}_{m_d} \otimes \cdots \otimes \hat{I}_{m_3} \otimes D_{x_2}^k \otimes \hat{I}_{m_1}, & \cdots, & D_{x_d}^k \otimes \hat{I}_{m_{d-1}} \otimes \cdots \otimes \hat{I}_{m_1} \end{bmatrix},$$

with D_r^k, $r = x_1, \cdots, x_d$, the 1D divergence operator of order k on the r-axis [5, p. 5].

2.3.5 The discrete analog

In addition, since in the mimetic differences of any order k, the discrete scalar field U is defined on the staggered grid, needs to be interpolated, by an interpolation operator of order k, to the non-staggered grid, to be able to approximate $\int_U 1\,\nabla\cdot(w^TA_1w,\cdots,w^TA_dw)\,dX$, without loosing accuracy.

Hence, the mimetic approximation of order k for $\int_U 1\,\nabla\cdot(w^TA_1w,\cdots,w^TA_dw)\,dX$, is given by

$$< D^k_{x_1\cdots x_d}(\mathcal{I}^k_D\hat{w}),\mathbb{1} >_{\mathcal{Q}^k}= \mathrm{vec}^d_L(\mathcal{I}^k_D\hat{w})^T\mathcal{Q}^k(D^k_{x_1\cdots x_d})^T\mathrm{vec}_L(\mathbb{1}), \tag{9}$$

with $\hat{w} = (w^TA_1w,\cdots,w^TA_dw), \mathrm{vec}^d_L = (\mathrm{vec}_L,\cdots,\mathrm{vec}_L)$ (the vectorization operator d times), where the time dependence has been omitted to simplify the notation, and $\mathbb{1}$ is the constant one discrete scalar field on S.

Formula (9) holds because in mimetic 1D differences

$$< Dw, f >_Q =< QDw, f >=< w,(QD)^Tf >=< w, D^TQf >,$$

and since the 1D integration by parts property (for $w=\mathbb{1}$) implies

$$h\mathbb{1}^T(D^TQ)f = f_{N+1}-f_0 = (-1,0,\cdots,0,1)f,$$

or equivalently,

$$h\mathbb{1}^T(D^TQ) = (-1,0,\cdots,0,1),$$

and

$$hQD^T\mathbb{1} = (-1,0,\cdots,0,1)^T. \tag{10}$$

2.3.6 The energy preserving proof

A direct computation of $\mathcal{Q}^k(D^k_{x_1\cdots x_d})$ gives

$$\mathcal{Q}^kD^T_{x_1\cdots x_d} = \begin{bmatrix} \hat{I}^T_{m_d}\otimes\cdots\otimes\hat{I}^T_{m_2}\otimes Q^k_{m_1+2}{D^k_{x_1}}^T \\ \hat{I}^T_{m_d}\otimes\cdots\otimes\hat{I}^T_{m_3}\otimes Q^k_{m_2+2}{D^k_{x_2}}^T\otimes\hat{I}^T_{m_1} \\ \vdots \\ Q^k_{m_d+2}{D^k_{x_d}}^T\otimes\hat{I}^T_{m_{d-1}}\otimes\cdots\otimes\hat{I}^T_{m_1} \end{bmatrix}$$

and by using the properties of the Kronecker product and the vectorization operator, one gets

$$\begin{aligned}\mathcal{Q}^k(D^k_{x_1\cdots x_d})^T\mathrm{vec}_L(\mathbb{1}) &= \begin{bmatrix} (\hat{I}^T_{m_d}\otimes\cdots\otimes\hat{I}^T_{m_2}\otimes Q^k_{m_1+2}{D^k_{x_1}}^T)\mathrm{vec}_L(\mathbb{1}) \\ (\hat{I}^T_{m_d}\otimes\cdots\otimes\hat{I}^T_{m_3}\otimes Q^k_{m_2+2}{D^k_{x_2}}^T\otimes\hat{I}^T_{m_1})\mathrm{vec}_L(\mathbb{1}) \\ \vdots \\ (Q^k_{m_d+2}{D^k_{x_d}}^T\otimes\hat{I}^T_{m_{d-1}}\otimes\cdots\otimes\hat{I}^T_{m_1})\mathrm{vec}_L(\mathbb{1}) \end{bmatrix} \\ &= \begin{bmatrix} \mathrm{vec}_L(Q^k_{m_1+2}D^k_{x_1})^T\mathbb{1}_{m_1+2,(m_2+2)\cdots(m_d+2)}(\hat{I}_{m_d}\otimes\cdots\otimes\hat{I}_{m_2}) \\ (\hat{I}^T_{m_d}\otimes\cdots\otimes\hat{I}^T_{m_3}\otimes Q^k_{m_2+2}{D^k_{x_2}}^T\otimes\hat{I}^T_{m_1})\mathrm{vec}_L(\mathbb{1}) \\ \vdots \\ (Q^k_{m_d+2}{D^k_{x_d}}^T\otimes\hat{I}^T_{m_{d-1}}\otimes\cdots\otimes\hat{I}^T_{m_1})\mathrm{vec}_L(\mathbb{1}) \end{bmatrix},\end{aligned} \tag{11}$$

since $(B^T\otimes A)\mathrm{vec}_L(X)=\mathrm{vec}_L(AXB^T)$, with $\mathbb{1}_{p,q}$ is a $p\times q$ matrix of ones.

From (10)

$$\begin{aligned}Q^k_{m_1+2}{D^k_{x_1}}^T\mathbb{1}_{m_1+2,\frac{m}{m_1+2}} &= \begin{bmatrix} -1 & \cdots & -1 \\ 0 & \cdots & 0 \\ \vdots & \vdots & \vdots \\ 0 & \cdots & 0 \\ 1 & \cdots & 1 \end{bmatrix}_{(m_1+1)\times\frac{m}{m_1+2}} \\ &= [-1,0,\cdots,0,1]^T_{m_1+1}[1,\cdots,1]_{\frac{m}{m_1+2}}.\end{aligned} \tag{12}$$

By (12), if $M=[Q^k_{m_1+2}{D^k_{x_1}}^T\mathbb{1}_{m_1+2,\frac{m}{m_1+2}}](\hat{I}_{m_d}\otimes\cdots\otimes\hat{I}_{m_2})$, one obtains

$$\begin{aligned}M &= \begin{bmatrix} -1 & \cdots & -1 \\ 0 & \cdots & 0 \\ \vdots & \vdots & \vdots \\ 0 & \cdots & 0 \\ 1 & \cdots & 1 \end{bmatrix}_{(m_1+1)\times\frac{m}{m_1+2}} (\hat{I}_{m_d}\otimes\cdots\otimes\hat{I}_{m_2}) \\ &= \begin{bmatrix} -1 & \cdots & -1 \\ 0 & \cdots & 0 \\ \vdots & \vdots & \vdots \\ 0 & \cdots & 0 \\ 1 & \cdots & 1 \end{bmatrix}_{(m_1+1),\frac{m_0}{m_1}} = [-1,0,\cdots,0,1]^T_{m_1+1}[1,\cdots,1]_{\frac{m_0}{m_1}},\end{aligned} \tag{13}$$

where $m_0 = m_1 \cdots m_d$, and hence $[Q^k_{m_1+2} {D^k_{x_1}}^T \mathbb{1}_{m_1+2,\frac{m}{(m_1+2)}}](\hat{I}_{m_d} \otimes \cdots \otimes \hat{I}_{m_2})$ is the boundary information of faces $\{-1\} \times N_{m_2} \times \cdots N_{m_d}$ (with negative sign) and $\{1\} \times N_{m_2} \times \cdots \times N_{m_d}$ (with positive sign).

Since $A \otimes B = P_l(B \otimes A)P_r$, for some permutation matrices P_l and P_r, then the remaining rows other than the first of (11) become

$$\begin{aligned}
(\hat{I}^T_{m_d} \otimes \cdots \otimes \hat{I}^T_{m_3} \otimes Q^k_{m_2+2} {D^k_{x_2}}^T \otimes \hat{I}^T_{m_1})\mathrm{vec}_L(\mathbb{1}) &= P^{(2)}_l(\hat{I}^T_{m_1} \otimes \hat{I}^T_{m_d} \otimes \cdots \otimes \hat{I}^T_{m_3} \otimes Q^k_{m_2+2} {D^k_{x_2}}^T)P^{(2)}_r \mathrm{vec}_L(\mathbb{1}), \\
&\vdots \\
(Q^k_{m_d+2} {D^k_{x_d}}^T \otimes \hat{I}^T_{m_{d-1}} \otimes \cdots \otimes \hat{I}^T_{m_1})\mathrm{vec}_L(\mathbb{1}) &= P^{(d)}_l(\hat{I}^T_{m_{d-1}} \otimes \cdots \otimes \hat{I}^T_{m_1} \otimes Q^k_{m_d+2} {D^k_{x_d}}^T)P^{(d)}_r \mathrm{vec}_L(\mathbb{1}),
\end{aligned} \tag{14}$$

for some matrices $P^{(2)}_l, P^{(2)}_r, \cdots, P^{(d)}_l, P^{(d)}_r$, respectively.

As $\mathrm{vec}_L(\mathbb{1})$ is a vector of only ones, then $P^{(p)}_r \mathrm{vec}_L(\mathbb{1}) = \mathrm{vec}_L(\mathbb{1})$, $p = 2, \cdots, d$. Hence,

$$\begin{aligned}
(\hat{I}^T_{m_d} \otimes \cdots \otimes \hat{I}^T_{m_3} \otimes Q^k_{m_2+2} {D^k_{x_2}}^T \otimes \hat{I}^T_{m_1})\mathrm{vec}_L(\mathbb{1}) &= P^{(2)}_l \mathrm{vec}_L(Q^k_{m_2+2} {D^k_{x_2}}^T \mathbb{1}_{m_2+2,\frac{m}{m_2+2}}(\hat{I}_{m_1} \otimes \hat{I}_{m_3} \otimes \cdots \otimes \hat{I}_{m_d})), \\
&\vdots \\
(Q^k_{m_d+2} {D^k_{x_d}}^T \otimes \hat{I}^T_{m_{d-1}} \otimes \cdots \otimes \hat{I}^T_{m_1})\mathrm{vec}_L(\mathbb{1}) &= P^{(d)}_l \mathrm{vec}_L(Q^k_{m_d+2} {D^k_{x_d}}^T \mathbb{1}_{m_d+2,\frac{m}{m_d+2}}(\hat{I}_{m_{d-1}} \otimes \cdots \otimes \hat{I}_{m_1})),
\end{aligned} \tag{15}$$

respectively.

Similar arguments to those for the first row of (11) demonstrate that

$$Q^k_{m_i+2} {D^k_{x_i}}^T \mathbb{1}_{m_i+2,\frac{m}{m_i+2}} = [-1, 0, \cdots, 0, 1]^T_{m_i+1} [1, \cdots, 1]_{\frac{m}{m_i+2}}, \quad i = m_2, \cdots, m_d,$$

and hence, the i-th row, $i = 1, \cdots, d$, of (11) is the boundary information of faces $N_{m_1} \times \cdots \times N_{m_{i-1}}\{-1\} \times N_{m_{i+1}} \times \cdots \times N_{m_d}$ (with negative sign) and $N_{m_1} \times \cdots \times N_{m_{i-1}}\{1\} \times N_{m_{i+1}} \times \cdots \times N_{m_d}$ (with positive sign).

Therefore, (9) becomes

$$
\begin{aligned}
h\left[\left(\mathrm{vec}_L^d(\mathcal{I}_D^k\hat{w})\right)^T\right]\mathcal{Q}^k D_{x_1\cdots x_d}^T \mathrm{vec}_L(\mathbb{1}) &= \\
h\left(\mathrm{vec}_L^d(\mathcal{I}_D^k(w^TA_1w|\cdots|w^TA_dw)^T\right)^T &\cdot \\
\begin{bmatrix}
[-1,0,\cdots,0,1]_{m_1+1}^T[1,\cdots,1]_{\frac{m_0}{m_1}} \\
P_l^{(2)}[-1,0,\cdots,0,1]_{m_2+1}^T[1,\cdots,1]_{\frac{m_0}{m_2}} \\
\vdots \\
P_l^{(d)}[-1,0,\cdots,0,1]_{m_d+1}^T[1,\cdots,1]_{\frac{m_0}{m_d}}
\end{bmatrix} &= \\
h\Big\{\mathrm{vec}_L^d((w^TA_1w|\cdots|w^TA_dw)\mathcal{I}_D^{k\,T})^T[-1,0,\cdots,0,1]_{m_1+1}^T[1,\cdots,1]_{\frac{m_0}{m_1}} &+ \\
\mathrm{vec}_L^d((w^TA_1w|\cdots|w^TA_dw)\mathcal{I}_D^{k\,T})^T[-1,0,\cdots,0,1]_{m_1+1}^T P_l^{(2)}[-1,0,\cdots,0,1]_{m_2+1}^T[1,\cdots,1]_{\frac{m_0}{m_2}} &+ \\
\vdots & \\
\mathrm{vec}_L^d((w^TA_1w|\cdots|w^TA_dw)\mathcal{I}_D^{k\,T})^T[-1,0,\cdots,0,1]_{m_1+1}^T P_l^{(d)}[-1,0,\cdots,0,1]_{m_d+1}^T[1,\cdots,1]_{\frac{m_0}{m_d}}\Big\} &= \\
h\sum_{i=1}^{d}\sum_{J_i}(w^TA_iw|_{(s_{j_1},\cdots,s_{j_{i-1}},1,s_{j_{i+1}},\cdots,s_{j_d},t)} - w^TA_iw|_{(s_{j_1},\cdots,s_{j_{i-1}},-1,s_{j_{i+1}},\cdots,s_{j_d},t)}),&
\end{aligned}
$$

where

$$
\sum_{J_i} = \sum_{j_1=1}^{m_1+1}\cdots\sum_{j_{i-1}=1}^{m_{i-1}+1}\sum_{j_{i+1}=1}^{m_{i+1}+1}\cdots\sum_{j_d=1}^{m_d+1}.
$$

Therefore, the mimetic discrete analog of (8) is given by

$$
\begin{aligned}
\mathcal{E}(T) + h\sum_{i=1}^{d}\sum_{J_i} w^TA_iw|_{(s_{j_1},\cdots,s_{j_{i-1}},1,s_{j_{i+1}},\cdots,s_{j_d},t)} &= \\
\mathcal{E}(0) + h\sum_{i=1}^{d}\sum_{J_i} g_i^T(s_{j_1},\cdots,s_{j_{i-1}},s_{j_{i+1}},\cdots,s_{j_d},t)A_ig_i(s_{j_1},\cdots,s_{j_{i-1}},s_{j_{i+1}},\cdots,s_{j_d},t),&
\end{aligned}
$$

i.e., the energy at T plus the energy lost at the front boundaries matches the initial energy plus the energy gained at the back boundaries.

2.4 Case II: A nonlinear conservation law

Consider the following initial/boundary problem for nonlinear scalar conservation law in one space dimension

$$\begin{aligned} u_t + (F(u))_x &= 0, && (x,t) \in [-1,1] \times (0,T), && (16)\\ u(-1,t) &= u(1,t), && t \in (0,T), && (17)\\ u(x,0) &= g(x), && (x,t) \in [-1,1] \times \{t=0\}. && (18) \end{aligned}$$

with periodic boundary conditions.

Multiplying (16) by u and integrating by parts over $[-1,1]$, one gets

$$\begin{aligned} 0 &= \int_{-1}^{1} u\, u_t\, dx + \int_{-1}^{1} u\, (F(u))_x\, dx \\ &= \int_{-1}^{1} \frac{d}{dt}\left(\frac{1}{2}\, u^2\right) dx + [u\, F(u)]_{-1}^{1} - \int_{-1}^{1} u_x\, F(u)\, dx \\ &= \frac{1}{2}\, \frac{d}{dt}\left(\int_{-1}^{1} u^2\, dx\right) - \int_{-1}^{1} F(u)\, u_x\, dx, \end{aligned}$$

since, in the second identity, the middle term vanishes due to the periodic boundary conditions.

After integrating from 0 to T, it follows that

$$2\int_0^T \int_{-1}^{1} F(u)\, u_x\, dx\, dt = E(T) - E(0). \tag{19}$$

where $E(t) = \int_{-1}^{1} u^2(x,t)\, dx$, is the total energy of u at time t.

If $F = \frac{dH}{dx}$ then

$$\int_{-1}^{1} F(u)\, u_x\, dx = \int_{-1}^{1} H^{'}(u)\, u_x\, dx = \int_{-1}^{1} (H(u))_x\, dx,$$

whose mimetic discrete analog of order of accuracy $k = 2, 4, 6, 8$, for $U = U(x,t)$ the discrete version of $u(x,t)$ at center cells, is

$$\begin{aligned} h\langle DI_D(H(U)), \mathbb{1}\rangle_Q &= h\langle I_D(H(U)), QD^T\mathbb{1}\rangle = h(H(U))^T I_D^T(QD^T\mathbb{1}) \\ &= (H(U))^T I_D^T(-1,0,\cdots,0,1)^T = (H(U))^T(-1,0,\cdots,0,1)^T \\ &= H(U(1,t)) - H(U(-1,t)) = 0, \end{aligned}$$

because I_D is an interpolation operator, which has first row $(1,0,\cdots,0)$ and last row $((0,\cdots,0,1)$ (see [7]), the periodic boundary conditions and by formula (10).

If $\mathcal{E}(t)$ denotes the discrete energy of U then (19) becomes

$$\mathcal{E}(T) = \mathcal{E}(0).$$

If the boundary conditions are not periodic then for $F = \frac{dH}{dx}$ one has

$$\begin{aligned}\sum_{t_n} w_1(t_n)[H(U(1,t_n)) - H(U(-1,t_n))] - \frac{1}{2}(\mathcal{E}(T) - \mathcal{E}(0)) \quad = \\ \sum_{t_n} w_2(t_n)[U(1,t_n)\, F(U(1,t_n)) - U(-1,t_n)\, F(U(-1,t_n))]\end{aligned}$$

where w_1, w_2 are convenient quadrature weights, or equivalently

$$\begin{aligned}\frac{1}{2}\,\mathcal{E}(T) + \sum_{t_n\in[0,T]} w_2(t_n)(U(1,t_n)\, F(U(1,t_n))) - \sum_{t_n\in[0,T]} w_1(t_n)H(U(1,t_n)) \quad = \\ \frac{1}{2}\,\mathcal{E}(0) + \sum_{t_n\in[0,T]} w_2(t_n)(U(-1,t_n)\, F(U(-1,t_n))) - \sum_{t_n\in[0,T]} w_1(t_n)H(U(-1,t_n)).\end{aligned}$$

2.5 Case III: A nonlinear system of conservation laws

Consider the following initial/boundary problem for a system of c nonlinear conservation law in $V = [-1,1]^d \subset \mathbb{R}^d$

$$\begin{aligned}
w_t + \nabla\cdot F(w) &= 0, && (x,t) \in (-1,1)^d \times (0,T), && (20)\\
w(x_1,\cdots,x_d,0) &= w_0(x_1,\cdots,x_d), && x \in (-1,1)^d, && (21)\\
w(x_1,\cdots,x_{i-1},-1,x_{i+1},\cdots,x_d,t) &= g_i^-(\hat{x}_i,t), && (\hat{x}_i,t) \in [-1,1]^{d-1}\times[0,T], && (22)\\
w(x_1,\cdots,x_{i-1},1,x_{i+1},\cdots,x_d,t) &= g_i^+(\hat{x}_i,t), && (\hat{x}_i,t) \in [-1,1]^{d-1}\times[0,T], && (23)
\end{aligned}$$

in which

$$w = (w_1,\cdots,w_c), \qquad w_i = w_i(x_1,\cdots,x_d,t), \qquad i = 1,\cdots,c,$$

$w_0 : \mathbb{R}^d \to \mathbb{R}$ is the initial condition and we assume that the boundary functions

$$g_i^{\pm} : \mathbb{R}^{d-1}\times(0,\infty) \mapsto \mathbb{R}^c, \qquad i = 1,\cdots,d,$$

have spatial coordinates defined on $\hat{x}_i = (x_1,\cdots,x_{i-1},x_{i+1},\cdots,x_d)$, and that the flux is given by

$$F(w) = (F_1(w),\cdots,F_c(w))^T, \qquad F_i(w) = (F_{i1}(w),\cdots,F_{id}(w)), \qquad i = 1,\cdots,c.$$

Multiplying (20) by w and integrating by parts over $[-1,1]^d$, one gets

$$\begin{aligned} 0 &= \int_V w^T\, w_t\, dX + \int_V w^T (\nabla \cdot F(u))\, dX \\ &= \frac{1}{2}\frac{d}{dt}\left(\int_V w^T w\, dX\right) + \int_{\partial V} w^T (b\cdot F_1(w), \cdots, b\cdot F_c(w))\, dS - \int_V \sum_{i=1}^{d}\left(\frac{\partial w}{\partial x_i}\cdot F_i(w)\right) dX \end{aligned} \tag{24}$$

where $dX = dx_1 \cdots dx_d$, $b = (1, \cdots, 1) \in \mathbb{R}^d$.

Suppose that for each $1 \le i \le d$ there exists H_i such that $F_i = \nabla_w H_i$. In that case

$$\sum_{i=1}^{d}\left(\frac{\partial w}{\partial x_i}\cdot F_i(w)\right) = \sum_{i=1}^{d}\left(\frac{\partial w}{\partial x_i}\cdot \nabla H_i(w)\right) = \sum_{i=1}^{d}\sum_{j=1}^{c}\frac{\partial H_i}{\partial w_j}\frac{\partial w_j}{\partial x_i} = \sum_{i=1}^{d}\frac{\partial H_i}{\partial x_i} = \nabla_x \cdot H(w).$$

The mimetic discrete analog with order of accuracy $k = 2, 4, 6, 8$, of

$$\int_V \nabla_x \cdot H(w)\, dX$$

for $W = W(x,t)$, the discrete version of $w(x,t)$ at center cell, is

$$\begin{aligned} h\,\langle D_{x_1\cdots x_d}\mathcal{I}_D H(W), \mathbb{1}\rangle_{\mathcal{Q}} &= h\,\langle \mathcal{I}_D H(W), \mathcal{Q}D^T_{x_1\cdots x_d}\rangle = h\, H^T(W)\mathcal{I}_D^T(\mathcal{Q}D^T_{x_1\cdots x_d}\mathbb{1}) \\ &= H^T(W)\mathcal{I}_D^T \mathrm{vec}_L[(-1,0,\cdots,0,1)^d] = H^T(W)\mathrm{vec}_L[(-1,0,\cdots,0,1)^d] \\ &= \sum_{i=1}^{d} H_i(W(x_1,\cdots,x_{i-1},1,x_{i+1},\cdots,x_d)) \\ &- \sum_{i=1}^{d} H_i(W(x_1,\cdots,x_{i-1},-1,x_{i+1},\cdots,x_d)) \\ &= \sum_{i=1}^{d}(H_i(g_i^+(\hat{x}_i)) - H_i(g_i^-(\hat{x}_i))) = 0 \end{aligned}$$

for periodic boundary conditions.

In addition, for periodic boundary conditions

$$\begin{aligned}
\int_{\partial V} w^T(b\cdot F_1(w),\cdots,b\cdot F_c(w))\,dS &= \\
\sum_{i=1}^{d}\int_{[-1,1]^{d-1}} w^T(x_1,\cdots,x_{i-1},1,x_{i+1},\cdots,x_d) &\cdot \\
(b\cdot F_1(w(x_1,\cdots,x_{i-1},1,x_{i+1},\cdots,x_d),\cdots,b\cdot F_c(w(x_1,\cdots,x_{i-1},1,x_{i+1},\cdots,x_d))\,d\hat{X}_i &- \\
\sum_{i=1}^{d}\int_{[-1,1]^{d-1}} w^T(x_1,\cdots,x_{i-1},-1,x_{i+1},\cdots,x_d) &\cdot \\
(b\cdot F_1(w(x_1,\cdots,x_{i-1},-1,x_{i+1},\cdots,x_d),\cdots,b\cdot F_c(w(x_1,\cdots,x_{i-1},-1,x_{i+1},\cdots,x_d))\,d\hat{X}_i &= \\
\sum_{i=1}^{d}\int_{[-1,1]^{d-1}} g_i^+(\hat{x}_i)\cdot(b\cdot F_1(g_i^+(\hat{x}_i)),\cdots,b\cdot F_c(g_i^+(\hat{x}_i))) &- \\
\sum_{i=1}^{d}\int_{[-1,1]^{d-1}} g_i^-(\hat{x}_i)\cdot(b\cdot F_1(g_i^-(\hat{x}_i)),\cdots,b\cdot F_c(g_i^-(\hat{x}_i))) &= 0.
\end{aligned}$$

Therefore, after integrating (24) from 0 to T, it follows that

$$E(T) = E(0).$$

where $E(t) = \int_{[-1,1]^d} w^T(x,t)w(x,t)\,dx$, is the total energy of u at time t.

If $\mathcal{E}(t)$ denotes the discrete energy of U then (19) becomes

$$\mathcal{E}(T) = \mathcal{E}(0).$$

If the boundary conditions are not periodic then for $F = \frac{dH}{dx}$ one has

$$\begin{aligned}
\sum_{t_n} q_1(t_n)[H(U(1,t_n)) - H(U(-1,t_n))] - \frac{1}{2}(\mathcal{E}(T) - \mathcal{E}(0)) &= \\
\sum_{t_n} q_2(t_n)[U(1,t_n)\,F(U(1,t_n)) - U(-1,t_n)\,F(U(-1,t_n))]
\end{aligned}$$

where q_1, q_2 are high-order quadrature weights, or equivalently

$$\begin{aligned}
\frac{1}{2}\,\mathcal{E}(T) + \sum_{t_n\in[0,T]} q_2(t_n)(U(1,t_n)\,F(U(1,t_n))) - \sum_{t_n\in[0,T]} q_1(t_n)H(U(1,t_n)) &= \\
\frac{1}{2}\,\mathcal{E}(0) + \sum_{t_n\in[0,T]} q_2(t_n)(U(-1,t_n)\,F(U(-1,t_n))) - \sum_{t_n\in[0,T]} q_1(t_n)H(U(-1,t_n)).
\end{aligned}$$

3 Numerical example

Instead of providing examples for each of the cases where the energy preservation has been demonstrated in the previous sections, this paper focus on a more general nonlinear system of conservation laws, for which the solution is known.

Consider the 2D Euler equations [16, 19]

$$\frac{\partial q}{\partial t} + \nabla \cdot f = 0, \tag{25}$$

with

$$q = \begin{pmatrix} \rho \\ \rho\, u \\ \rho\, v \\ E \end{pmatrix}, \qquad f_1 = \begin{pmatrix} \rho\, u \\ \rho\, u^2 + p \\ \rho\, u\, v \\ (E+p)u \end{pmatrix}, \qquad f_2 = \begin{pmatrix} \rho\, v \\ \rho\, u\, v \\ \rho\, v^2 + p \\ (E+p)v \end{pmatrix},$$

where ρ is the density, u the horizontal velocity, v the vertical velocity, and E the total energy. The equations are closed by the ideal gas law

$$p = (\gamma - 1)\left(E - \frac{1}{2}\,\rho(u^2 + v^2)\right),$$

where γ is a fluid-dependent constant, which for typical atmospheric gases can be taken to be $\gamma = \frac{7}{5}$.

For a smooth exact solution, initially centered at (x_0, y_0) and convected at the constant velocity (u_0, v_0), one can consider an isentropic vortex given as

$$\begin{aligned} \rho &= \left(1 - \left(\frac{\gamma - 1}{16\gamma\pi^2}\right)\beta^2 e^{2(1-r^2)}\right)^{\frac{1}{\gamma-1}}, \\ u &= u_0 - \beta e^{(1-r^2)}\,\frac{y - y_0}{2\pi}, \\ v &= v_0 + \beta e^{(1-r^2)}\,\frac{x - x_0}{2\pi}, \\ p &= \rho^\gamma, \end{aligned}$$

or equivalently

$$E = \frac{\rho^\gamma}{\gamma - 1} + \frac{1}{2}\rho(u^2 + v^2),$$

where

$$r = \sqrt{(x - u_0 t - x_0)^2 + (y - v_0 t - y_0)^2}.$$

Assume a $[-5,5] \times [-5,5]$ 2D domain, with $\beta = 5.0$, and the initial position of the vortex and the initial convection velocity given by

$$x_0 = y_0 = 0, u_0 = 1, v_0 = 0.$$

We employed Corbino-Castillo fourth-order mimetic operators in conjunction with a second-order leapfrog scheme for the temporal discretization to resolve (25). The visual representation of our findings is illustrated in Figures 1 through 4, presenting the approximated solutions for the conserved quantities $(\rho, \rho u, \rho v, E)$ after 0.1 seconds. Figure 5 portrays the variation of each quantity over time; this is obtained by numerically integrating the solution surfaces at various stages.

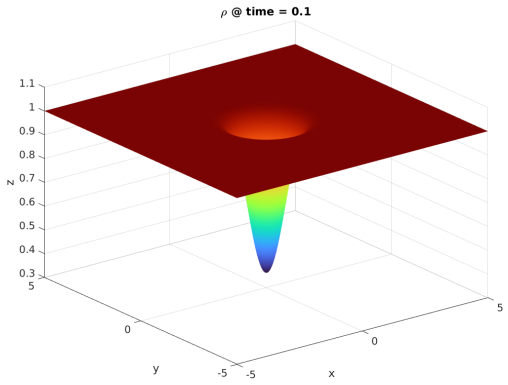

Figure 1: Density profile after 0.1 seconds.

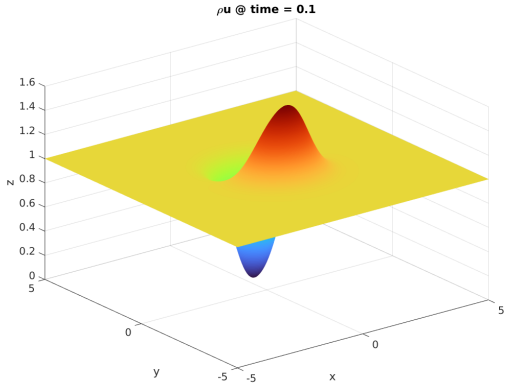

Figure 2: Momentum in the u-direction.

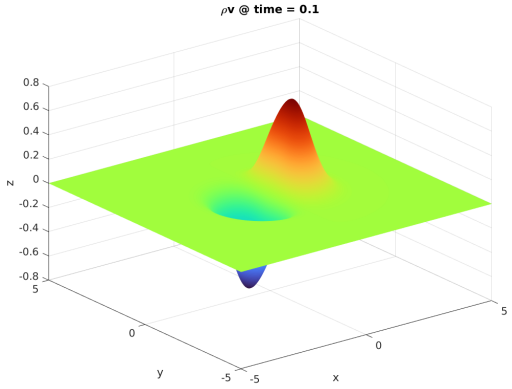

Figure 3: Momentum in the v-direction.

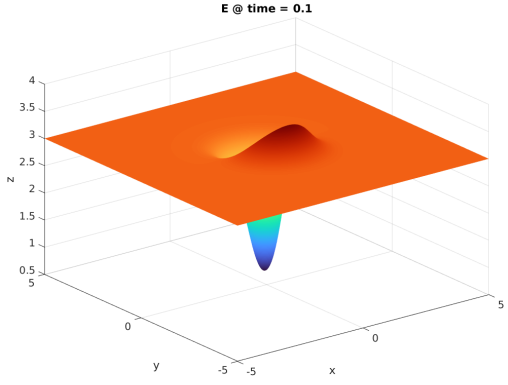

Figure 4: Total energy after 0.1 seconds.

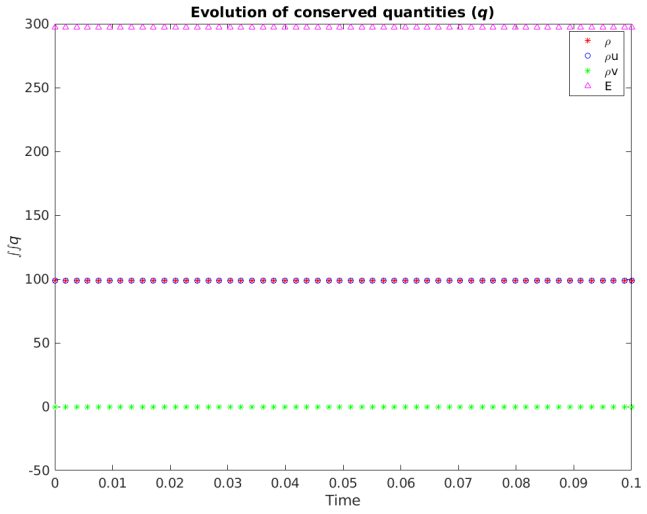

Figure 5: Variability of the four quantities of interest over time.

4 Conclusions

The first part of this work focused on demonstrating that symmetric hyperbolic systems of first-order PDEs, as well as, nonlinear or scalar systems of conservation laws, where the flux can be described as the gradient of some potential fields, are proven. The choice of these system of conservation laws is required to preserved the linearity of the algebra involved. It is worth to mention that the exact same proofs are valid for the Castillo-Grone mimetic differences, since that approach satisfy the same extended Gauss divergence theorem formula.

In the second part of this paper, it is numerically shown the energy preservation of the fourth-order Corbino-Castillo mimetic difference scheme when applied to systems of conservation laws. As illustrated by the numerical example, the mimetic-based solution converges to the exact solution of the problem while preserving all the quantities of interest. This practical validation strengthens the theoretical foundation of our approach.

References

[1] Arnold, D.N., Finite Element Exterior Calculus, SIAM, 2018.

[2] Boffi, D., Brezzi, F., Demkovicz, L.F., Durán, R.G., Falk, R.S., and Fortin, M. (eds), Mixed Finite Elements, Compatibility Conditions, and Applications, Lecture Nottes in Mathematics, vol. 39, Springer-Verlag, Berlin, Heildelberg, 2008.

[3] Castillo, J.E., and Grone, R.D., A matrix analysis approach to higher-order approximations for divergence and gradients satisfying a global conservation law, SIAM J. Matrix Anal. Appl., Vol. 25, No. 1, pp. 128-142, 2003.

[4] Castillo, J.E., and Miranda, G.F., Mimetic Discretization Method, CRC Press, Boca Raton, 2013.

[5] Corbino, J., and Castillo, J.E., High-order mimetic finite-difference operators satisfying the extended Gauss divergence theorem, J. Comput. Appl. Math., v. 364, 2020, 112326.

[6] Corbino, J., and Castillo, J.E., MOLE: Mimetic Operators Library Enhanced, CSRC Report Sep. 25, 2017.

[7] Dumett, M.A., and Castillo, J.E., Gradient and Divergence Corbino-Castillo Interpolation Operators, San Diego State University, CSRC Report, 5-Dec-2022.

[8] Dumett, M.A., and Castillo, J.E., Mimetic Differences Vector Calculus Identities, San Diego State University, CSRC Report, 13-Jul-2023.

[9] Dumett, M.A., and Castillo, J.E., Energy conservation and convergence of high-order mimetic schemes for the 3D advection equation, San Diego State University, CSRC Report, 21-Jul-2023.

[10] Dusinberre, G.M., Heat transfer calculations by numerical methods, Journal of the American Society for Naval Engineers, 67 (4), 991-1002, 1955.

[11] Dusinberre, G.M., Heat transfer calculation by finite differences, International Textbook Company, Scranton, Pennsylvania, 1961.

[12] Eldred, C., and Salinger, A., Structure-preserving numerical discretizations for domains with boundaries, Sandia National Laboratories, SAND2021-11517, September 2021, https://doi.org/10.2172/1820697.

[13] Eldred, C., and Stewart, J., Differential geometric approaches to momentum-based formulations for fluids, Sandia National Laboratories, SAND2022-12945, September 2022, https://doi.org/10.2172/1890065.

[14] Evans, L.C., Partial Differential Equations, Graduate Studies in Mathematics, Vol. 19, American Mathematical Society, Providence, Rhode Island, 1998.

[15] Kreeft, J., Palha, A., and Gerritsma, M., Mimetic Framework On Curvilinar Quadrilaterals Of Arbitrary Order arXiv:1111.4304v1 [math.NA], 2011, https://doi.org/10.48550/arXiv.1111.4304.

[16] J.S. Hesthaven, Numerical methods for conservation laws, SIAM Computational Science and Engineering, Philadelphia, Pennsylvania, 2018.

[17] Hirani, A.H., Discrete Exterior Calculus, California Institute of Technology, PhD thesis, 2003.

[18] Justo, D., High Order Mimetic Methods, VDM Verlag Dr. Müller Aktiengesellschaft & Co. KG, 2009.

[19] Kurganov, A., and Tadmor, E., Solution of Two-Dimensional Riemann Problems for Gas Dynamics without Riemann Problem Solvers, Numerical Methods for Partial Differential Equations, 18(5), pp 584-608, 2002.

[20] Marrone, M. Computational aspects of the cell methods in electrodynamics, In Teixeira, F.L. (ed.), Geometric Methods in Computational Electromagnetics, PIER 32, pp. 317-356, EMW Publishing, Cambridge, MA, 2001.

[21] Nicolaides, R.A., and Wu, X., Covolume solutions of the three-dimensional div-curl equations, SIAM J. Numer. Anal., 34 (6), 2195-2203, 1997.

[22] Olsson, P., Summation by parts, projections and stability, I., Math. Comput. 64 (211), 1035-1065, S23-S26, 1995.

[23] Olsson, P., Summation by parts, projections and stability, II., Math. Comput. 64 (212), 1473-1493, 1995.

[24] Robidoux, N., and Steinberg, S., A Discrete Vector Calculus in Tensor Grids, Computational Methods in Applied Mathematics, 11 (1), 23-66, 2011, https://doi.org/10.2478/cmam-2011-0002.

[25] Shashkov, M., Conservative finite-difference methods on general grids, CRC Press, Boca Raton, FL, 1995.

[26] Strikwerda, J.C., Finite Difference Schemes and Partial Differential Equations, Second Edition, SIAM, Philadelphia, 2004.

[27] da Veiga, L.B., Lipnikov K., and Manzini, G., The mimetic finite difference method for elliptic problems, Springer International Publishing, Switzerland, 2014.

[28] Boada, A., Corbino J., and Castillo J.E., High Order Mimetic Difference Simulation of Unsaturated flow using Richard's Equation, Mathematics in Applied Science and Engineering, 2020 Vol 1, (4).

[29] Boada, A., Paolini, C. and Castillo J.E., High-Order Mimetic Finite Differences for Anisotropic Elliptic Equations, Computers and Fluids, 2020, 213.

[30] Rojas, O., Otero, B., Castillo, J.E., and Day, S.M., Low Dispersive Modeling of Rayleigh Waves on Partly-Staggered Grids, Journal of Computational Geosciences, 18:1, 29-43, 2014.

[31] Rojas, O., Dunham, E., Day, S., Dalguer, L., and Castillo, J.E., Finite Difference Modeling of Rupture Propagation with Strong Velocity-Weakening Friction, Geophysical Journal International Seismology, 179, 1831-1858, 2009.

[32] Rojas, O., Day, S., Castillo, J.E. and Dalguer, L.A., Modeling of Rupture Propagation using High-Order Mimetic Finite Differences, Geophysical Journal International Seismology, 172, 631-650, 2008.

[33] Córdova, L.J., Rojas, O., Otero, B., and Castillo, J.E., Compact finite difference modeling of 2-D acoustic wave propagation, Journal of Computational and Applied Mathematics, 2015 .

[34] De la Puente, J., Ferrer, M., Hanzich, M., Castillo, J.E., and Cela, J.M., Mimetic Seismic Wave Modeling Including Topography on Deformed Staggered Grids, Geophysics, 79, T125-T141, 2014.